Physics Opportunities of the Nuclear Excitation by Electron Capture Process*

Yi Yang,[1] Hanxu Zhang,[2] Yuanbin Wu,[3] Song Guo,[4] Xu Wang,[2,5] Changbo Fu,[1] Yang Sun,[6] and Yugang Ma[1]

[1]*Key Lab of Nuclear Physics and Ion-beam Application (MoE), Institute of Modern Physics, Fudan University, Shanghai 200433, China*
[2]*Graduate School, China Academy of Engineering Physics, Beijing 100193, China*
[3]*School of physics, Nankai University, Tianjin 300071, China*
[4]*Key Laboratory of High Precision Nuclear Spectroscopy, Institute of Modern Physics, Chinese Academy of Sciences, Lanzhou 730000, People's Republic of China*
[5]*Southern Center for Nuclear-Science Theory, Institute of Modern Physics, Chinese Academy of Sciences, Huizhou, Guangdong 516000, China*
[6]*School of Physics and Astronomy, Shanghai Jiao Tong University, Shanghai 200240, China*

Nuclear Excitation by Electron Capture (NEEC) stands as a fundamental process in nuclear physics, with its theoretical framework established nearly half a century ago. Despite its longstanding theoretical presence, experimental confirmation of NEEC remains elusive due to significant technical challenges. A notable effort to validate NEEC experimentally involved the enhanced ^{93m}Mo isomer depletion experiment, which was ultimately hindered by substantial noise interference. This mini-review provides a brief historical overview of NEEC studies and explores the role that NEEC processes play in astrophysical environments and laser-induced plasmas. To date, several platforms have been proposed to facilitate the observation of NEEC, including traditional cooling storage rings, ion accelerators, and electron beam ion traps. These approaches primarily aim to enhance the nuclear excitation rate, thereby improving the signal-to-noise ratio. Additionally, the potential of employing exotic vortex beams is described in this manuscript, proposing them as a novel methodological approach to address these challenges.

Keywords: NEEC, isomer, plasmas, accelerator

I. INTRODUCTION

Nuclear Excitation by Electron Capture (NEEC) is a process in which a positively charged ion captures a free electron, leading to the excitation of its nucleus. This intriguing process was first proposed by V. I. Goldanskii and V. A. Namiot in 1976, who explored its potential for observation in a laser-generated plasma of ^{235}U [1]. Originally referred to as inverse internal electron conversion, NEEC represents the inverse mechanism of internal conversion (IC) [2–4], as shown in Fig. 1.

The NEEC process holds profound significance across various fields, including astrophysics and nuclear physics. For instance, within astrophysical environments, this mechanism may influence nucleosynthesis. By elucidating nuclear mechanisms, including NEEC, in astrophysical plasmas, we can enhance our understanding of the formation, evolution, and interactions of stellar bodies, galaxies, and other astronomical entities [5]. Furthermore, NEEC is anticipated to serve as an important method for nuclear isomer production, with broad applications across various domains. These include nuclear medical treatment [6, 7], nuclear battery [8–10], nuclear clock [11, 12], and nuclear laser [13].

As a fundamental nuclear reaction process proposed nearly half a century ago but yet to be experimentally confirmed, NEEC has been the subject of extensive theoretical analyses and experimental proposals. These efforts encompass a range of methodologies, including the use of cooling storage rings [14], ion accelerators [15–19], electron beam ion traps (EBIT) [20], and others based on laser-induced plasma [7, 21–23].

The primary challenge in detecting NEEC lies in the presence of substantial background noise. As A. Pálffy et al. noted, by employing a Feshbach projection operator formalism to derive cross sections for various processes during electron capture [24], including NEEC, dielectronic recombination (DR) [25], and radiative recombination (RR) [26], notable DR and RR processes generate signals that closely mimic those from NEEC, thereby introducing significant background noise in experiments [27, 28]. This issue is particularly evident in experiments involving the isomer ^{93m}Mo, where a significant discrepancy exists between theoretical predictions and experimental results. Signals initially attributed to NEEC were later suspected to have originated from other mechanisms [17, 18, 29–32].

In addition to the basic NEEC process, several variants have been extensively explored in the literature. These include NEEC with X-rays (NEECX) [33], NEEC in Excited Ions (NEEC-EXI) [34, 35], and NEEC with vortex beams [36]. NEECX involves the capture of an electron into an

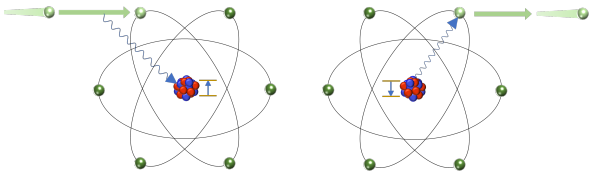

Fig. 1. Schematic diagrams of the NEEC (left) and IC (right) processes, which are inverse processes of each other.

* This work is supported by the National Key R&D Program of China (No. 2023YFA1606900) and the National Natural Science Foundation of China (NSFC) under Grant (No. 12235003).

excited atomic orbital, rather than the ground state, followed by the emitting of an X-ray photon [33]. This process facilitates the possibility of coincidence measurements by simultaneously detecting the x-photon and γ-photon. NEEC-EXI, on the other hand, represents the process where an electron is captured to an inner-shell vacancy in an atom that is already in an excited state [34].

NEEC with vortex electron beams introduces additional intriguing features to the study of NEEC. Vortex beams, distinguished by their helical wave fronts, carry intrinsic orbital angular momentum (OAM) along the direction of propagation [37–41]. This intrinsic OAM of vortex states introduces a new degree of freedom compared to plane-wave states, offering novel opportunities in the study of nuclear excitation processes by introducing new selection rules for nuclear processes. Since the initial proposal of optical vortex beams in Ref. [42], optical vortices have garnered significant interest, leading to a plethora of remarkable achievements and applications. Vortex photons have been intensively studied in contexts such as quantum communications, nonlinear optics, optical trapping, microscopy, nanotechnology, astrophysics, and manipulations of atomic transitions [37, 38, 43, 44]. In the context of NEEC, the use of electron vortex beams is anticipated to enhance the cross section by up to 4 orders of magnitude, presenting an opportunity for advancing this area of research [36].

In short, NEEC provides a quantum many-body platform that involves the interplay between atomic and nuclear systems. Despite its fundamental nature, it remains a process that is not yet fully understood. In this mini-review, we begin with a historical overview of the theoretical work of NEEC, followed by an examination of the role of NEEC within astrophysical environments and laser-induced plasmas. Additionally, the current status of NEEC studies using vortex beams and traditional accelerators will also be introduced. A brief comment on the proposed methods is given at the end as a summary.

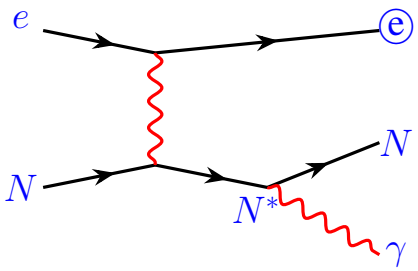

Fig. 2. The Feynman diagrams of the NEEC process. The "ⓔ" indicates that the electron is in an atomically bound state, while "e" denotes an electron in a continuum state. "N" represents the nucleus in its ground state, and "N^*" indicates the nucleus in an excited state.

II. THEORETICAL CROSS SECTION CALCULATION OF NEEC

In the theoretical treatment of the NEEC process, one considers the capture of a free electron into a bound state by a positively charged ion, which leads to the excitation of the nucleus. Typically, a γ-photon is emitted as follows. A Feynman diagram illustrating this process is given in Fig. 2, involving two steps and three states. The initial state is represented by $|i\rangle = |\boldsymbol{p}m_s, I_i M_{I_i}, n_{\boldsymbol{k}\sigma} = 0\rangle$, where $\boldsymbol{p}$ denotes the momentum of the free electron and m_s its spin in the z-direction. The nucleus is in its ground state with angular momentum I_i and z-component M_{I_i}. The term $n_{\boldsymbol{k}\sigma} = 0$ indicates the absence of photons. The intermediate state, $|d\rangle = |nl_{j_d}, I_d M_{I_d}, n_{\boldsymbol{k}\sigma} = 0\rangle$, features the electron captured into the orbital nl_{j_d} and the nucleus in the excited state $|I_d, M_{I_d}\rangle$, with no photons present. The final state, $|f\rangle = |nl_{j_d}, I_i M_{I_i}, n_{\boldsymbol{k}\sigma} = 1\rangle$, depicts the electron remaining in the orbital nl_{j_d}, the nucleus returned to its ground state $|I_i, m_{I_i}\rangle$, and the emission of photons, where $n_{\boldsymbol{k}\sigma}$ is the number of photons with polarization $\sigma = \pm 1$ and wave vector $\boldsymbol{k}$.

In this treatment, the nuclear excitation results from the action of a time-dependent electromagnetic field acting on the nucleus. Typically, the influence of this field is minimal and can be effectively addressed using first-order quantum-mechanical perturbation theory. The excitation probability can be expressed in terms of the same nuclear matrix elements that govern radiative transitions between nuclear states. More detailed illustrations of the main physical features of the process are provided in Ref. [24]. We will present the mathematical results of the quantum-mechanical theory for NEEC process in the following discussion.

The cross sections of the NEEC process for a free electron with kinetic energy ε are expressed as follows [24],

$$\sigma_{i\to d\to f} = \frac{2\pi^2}{p^2}\frac{A_r^{d\to f} Y_n^{i\to d}}{\Gamma}\mathcal{L}(\varepsilon - \varepsilon_0), \tag{1}$$

where $p^2c^2 = \varepsilon^2 + 2\varepsilon m_e c^2$ defines the momentum of the free electron. Given that NEEC is a resonant process, a Lorentz profile is essential,

$$\mathcal{L}(\varepsilon - \varepsilon_0) = \frac{\Gamma/2\pi}{(\varepsilon - \varepsilon_0)^2 + \frac{1}{4}\Gamma^2}. \tag{2}$$

The resonance energy ε_0 is determined by $\varepsilon_0 = \Delta E - E_b$, where ΔE is the transition energy of the nucleus, and E_b is the absolute value of the binding energy of the orbital nl_{j_d}. The width of the excited level Γ is given by,

$$\Gamma = A_r^{d\to f} + \frac{2I_d + 1}{2I_i + 1} Y_n^{i\to d}, \tag{3}$$

which comprises the electron capture rate $Y_n^{i\to d}$ and the photon emission rate $A_r^{d\to f}$, representing the reaction rates for the steps of excitation and de-excitation, respectively.

As previously noted, electromagnetic excitation involves the same nuclear matrix elements as the radiative transitions

of corresponding multipole order. Thus, for a given multipolarity λL with $\lambda = \mathrm{E/M}$, the photon emitting rates A_r are determined by the reduced transition matrix elements,

$$A_r = \frac{8\pi(L+1)}{L[(2L+1)!!]^2}\frac{\varepsilon^{2L+1}}{c}B\downarrow(\lambda L, I_d \to I_f), \quad (4)$$

as shown in Ref. [45], where $B\downarrow$ is the reduced nuclear transition probability for the decay. The electric (EL) and magnetic (ML) components of the electron capture rates Y_n are given by [46],

$$\begin{aligned} Y_n^{(\mathrm{EL})} &= \frac{4\pi^2\rho_i}{(2L+1)^2}B\uparrow(\mathrm{E}L, I_i \to I_d)(2j_d+1) \\ &\quad \times \sum_\kappa |R^{(\mathrm{E})}_{L,\kappa_d,\kappa}|^2 C(j_d L j; \frac{1}{2}0\frac{1}{2})^2, \quad (5) \\ Y_n^{(\mathrm{ML})} &= \frac{4\pi^2\rho_i}{L^2(2L+1)^2}B\uparrow(\mathrm{M}L, I_i \to I_d)(2j_d+1) \\ &\quad \times \sum_\kappa |R^{(\mathrm{M})}_{L,\kappa_d,\kappa}|^2 (2j+1)(\kappa_d+\kappa)^2 \begin{pmatrix} j_d & j & L \\ \frac{1}{2} & \frac{1}{2} & 0 \end{pmatrix}^2, \quad (6) \end{aligned}$$

where ρ_i is the density of initial electronic states. The relation of the reduced transition probability between the excitation $B\uparrow$ and the decay $B\downarrow$ of the nuclear state is given by $B\uparrow(\lambda L, I_i \to I_d) = \frac{2I_d+1}{2I_i+1}B\downarrow(\lambda L, I_d \to I_i)$. Other parameters, including j_d, j, and κ, relate to the electron orbital nl_{j_d}. The radial integrals involved in these calculations are given by [46],

$$R^{(E)}_{L,\kappa_d,\kappa} = \int_0^\infty dr\, r^{-L+1}\left(f_{n_d\kappa_d}f_{\varepsilon\kappa} + g_{n_d\kappa_d}g_{\varepsilon\kappa}\right), \quad (7)$$

$$R^{(M)}_{L,\kappa_d,\kappa} = \int_0^\infty dr\, r^{-L+1}\left(g_{n_d\kappa_d}f_{\varepsilon\kappa} + f_{n_d\kappa_d}g_{\varepsilon\kappa}\right), \quad (8)$$

where $f_{\varepsilon\kappa}(r)$ and $g_{\varepsilon\kappa}(r)$ in the integrals are components of the partial-wave expansion of the continuum electronic wave function. These functions $f_{n_d\kappa_d}(r)$ and $g_{n_d\kappa_d}(r)$, representing the bound electronic states, can be computed using atomic codes such as GRASP92 and AMBiT, among others.

III. NEEC IN ASTROPHYSICAL ENVIRONMENTS

The NEEC process could significantly impact astrophysical plasmas by altering the proportion of nuclear isomers present, similar to the influence of other nuclear reactions [47]. Its effects might vary with the temperature of plasmas, which influences the electron energy distribution. Further research is required to clarify the role of NEEC in these environments and to understand its potential impacts on the behavior and evolution of astrophysical plasmas.

A. NEEC in astrophysical plamsa

The role that NEEC plays in cosmic nucleosynthesis is not yet well understood. Astrophysical nucleosynthesis calculations depend on accurate nuclear reaction rate inputs, and NEEC cross sections could be critical for certain nuclear reactions within astrophysical plasmas. By considering nucleosynthesis as a network of reactions, it is crucial to recognize that a single reaction rate can profoundly influence astrophysical evolution. It is suspected that NEEC may significantly impact the production of isomers, thereby influencing nucleosynthesis processes.

A nuclear isomer is an excited state where structural effects within the nucleus inhibit its decay, granting the isomeric state potentially much longer lifetime than those of ordinary nuclear states. Known nuclear isomers exhibit a remarkable range of lifetimes, spanning from 10^{15} years for ^{180m}Ta—exceeding the widely accepted age of the universe—to as short as approximately 1 nanosecond, as is commonly recognized [48, 49]. From the perspective of isomer types, while shape isomers, spin traps, and seniority isomers tend to be concentrated in narrow mass regions on the nuclear chart, K-isomers are more broadly distributed, particularly in heavy and well-deformed nuclei [50].

Isomers are noteworthy not only for their unique intrinsic properties but also for their potential practical applications. The energy density of conventional energy sources, which rely on chemical processes, is fundamentally limited by the energy stored in chemical bonds—the so-called "chemical limit". To transcend this limit, it is necessary to explore the subatomic realm. Particularly interesting are nuclear isomers with half-lives of approximately one year or more. When energy is required, the reduction of the isomer population can be induced by providing the appropriate energy to excite the nucleus from the isomer to a higher state (referred to as the triggering level) and then allow it to decay to the ground state via paths that bypass the isomer [51–53]. This process results in the release of energy on a much shorter timescale than the natural decay of the isomers. Among the proposed triggering processes, the triggering of long-lived nuclear isomeric states via coupling to the atomic shells in the process of NEEC has attracted significant interest [14].

Low-lying triggering levels are desirable for obtaining high energy gain [54]. Identifying suitable triggering levels above the isomer is crucial to facilitate decay. For instance, most isomers, such as the 103.00 keV isomer in ^{81}Se, predominantly transition to lower-energy states, with transitions to the ground state occurring 99.949% of the time [55]. A sufficient connection to the ground state ensures that the destruction of the isomer does not deviate from thermal equilibrium. Historically, depletion of ^{178m2}Hf by low-energy (about 10 keV) photons was claimed by Collins and coworkers [56], but this was subsequently refuted by more sensitive measurements [57, 58]. Thus, while an isomer with a long lifetime may prevent thermalization at low temperatures, in a hotter environment, thermally driven transitions through intermediate states can enable equilibration.

Additionally, some isomers that are isolated from the ground state in the astrophysical sites where they are produced are not populated during the production of the nucleus. Thus, while some isomers play an influential role in astrophysical nucleosynthesis, most do not. This distinction leads to the definition of "astrophysical isomers", or "astromers" — nuclear isomers that have a significant influence in a specific astrophysical environment. Unlike their associated ground states, astromers behave differently and should be treated as separate species within nucleosynthesis networks. These networks may involve transitions that create and destroy these states.[59].

In astronomical environments, dynamics are governed by a multitude of microscopic processes, including electromagnetic processes such as ionization and radiative recombination, as well as nuclear reaction processes. The first two are crucial for maintaining charge balance and primarily occur between electrons and ions. Meanwhile, nuclear reaction processes may involve not only nuclei but also atoms, as seen in the case of NEEC. Cosmic plasmas are created through ionization, which can occur in several ways: collisions of fast particles with atoms, photoionization by electromagnetic radiation, or electrical breakdown in strong electric fields. The charge state of the plasma is determined by the balance between ionization and recombination, with radiative recombination making a significant contribution. Free electrons, abundant in astrophysical environments, are fundamental to the NEEC process. Thus, NEEC potentially plays a crucial role in nuclear excitation through electromagnetic interactions between electrons and ions during the recombination process.

In the context of cosmic nucleosynthesis, numerous nuclear interactions contribute to the production of elements. The majority of hydrogen (H) and helium (He), along with a small amount of lithium (Li), were formed during the first three minutes following the Big Bang. This early element formation is a key aspect of Big Bang Nucleosynthesis (BBN) [60–63], where heavier elements necessary for the formation of complex matter, including organic matter and life, are predominantly produced through fusion processes. Additionally, isotopes of elements heavier than iron (Fe) are primarily synthesized via neutron-capture processes (n-capture), including both slow (s) and rapid (r) neutron capture mechanisms. This is due to the strong Coulomb barrier that prevents their formation by fusion alone [60, 64–66].

The potential role of NEEC in depleting or accumulating isomeric states within highly charged ions in dense stellar plasmas, particularly in the context of the s-process, has attracted significant attention[47, 67–69]. During the s-process, a seed nucleus undergoes neutron capture to form an isotope with one higher atomic mass, followed by beta decay if it is unstable. Notably, nuclei along the s-process path tend to remain in isomeric states when the condition $\tau_\beta \ll \tau_n$ is met, where τ_β is beta decay lifetime, and τ_n is the time scale to capture an extra neutron. Hyoyin Gan *et al.* have concluded that NEEC should play a significant role in depleting the isomeric states of ^{58m}Co, ^{121m}Sb, and ^{152m}Eu by providing an effective isomer depletion channel [69].

Beyond simply affecting isomeric depletion, any nuclear reaction chain involving an intermediate isomeric state could be impacted by the NEEC process. Take, for example, the $A - i - B$ reaction sequence, where i represents an isomeric state. NEEC adds a new dimension by introducing an additional reaction step, $A - i - j - B$, where $i - j$ symbolizes the NEEC-induced excitation of the isomeric state i before it decays. This could potentially affect reactions such as ^{57}Co$-^{58m1}$Co$(-^{58m2}$Co$)-^{58}$Co [69].

NEEC is especially advantageous in extremely hot plasmas, which are better settings where NEEC can significantly influence nuclear reactions. This is because the reaction rate of NEEC increases as the charge states of ions increase [24]. Therefore, when performing astrophysical nucleosynthesis calculations, it is essential to incorporate the NEEC rates (λ_{NEEC}) for ions with zero, one, or two initially bound electrons into the nuclear reaction rate inputs.

To put it succinctly, viewing nucleosynthesis as just a series of interconnected reactions might be too simplistic. Recognizing that a single reaction rate, including NEEC, can have a profound impact on astrophysical evolution is vital. NEEC is suspected to significantly impact both the accumulation and depletion of isomers, thereby playing a pivotal role in nucleosynthesis.

B. Nuclear structure models for $B(\pi L)$

In the NEEC process, identifying the NEEC rate hinges on understanding the transition probabilities from the isomer to the triggering level [24]. These probabilities, which are crucial for evaluating the efficiency of triggering, depend on both the nuclear transition selection rules and the structural characteristics of the isomer and triggering level. If these transition probabilities haven't been measured experimentally, they must be estimated using reliable nuclear structure model calculations.

For instance, in the case of the $21/2^+$ isomer in ^{93}Mo (with an excitation energy $E_x = 2.425$ MeV and a half-life $\tau = 6.85$ hours), the critical transition to trigger the isomer is identified to be the E2 transition connecting the $21/2^+$ isomer to the upper $17/2^+$ level. This level, lacking experimental data, was predicted to have a substantial transition probability of 3.5 W.u. by Hasegawa *et al.* through nuclear shell model calculations. Consequently, it was concluded that there is a substantial prospect for observing induced isomer deexcitation if the $17/2^+$ level as the triggering level can be properly populated [70]. Indeed, subsequent experimental and theoretical discussions [17, 31, 32, 71, 72] have significantly relied on this transition probability.

To adequately account for the structure of the isomer and triggering levels in discussions, theories aiming to calculate NEEC cross sections must incorporate dedicated nuclear structure models. This critical integration of NEEC theory with modern nuclear structure models, which would enable a microscopic description of the interaction between nuclear

and atomic levels, remains an unfulfilled need. Among existing modern structure models, the nuclear shell model is the preferred choice [73–75].

The shell model provides a powerful framework for detailed nuclear structure studies, crucial for understanding nuclear isomers and their impacts under various conditions. This is because the theoretical states in these calculations must be eigenstates of the basic quantum numbers, such as angular momentum, parity, and isospin, given that all nuclear transitions occur between initial and final states with well-defined quantum numbers. Shell-model calculations typically require substantial computational resources. Thus, a minimal set of basis states that adequately captures the essential physics is sought. For nuclei that are neither heavy nor strongly deformed, only a limited number of single-particle states participate in defining the low-energy structure. In such cases, the conventional spherical shell model can leverage the reduced basis to compute relevant quantities efficiently. Upon completion of these calculations, it is expected that all levels, including isomers and triggering states, and the transitions among them are described consistently within the designated model spaces.

Except for nuclei near shell closures, the majority of nuclei on the nuclear chart exhibit deformed, posing a significant challenge to conventional spherical shell model due to the inevitable issue of dimensional explosion. Consequently, the exploration of nuclear structure in heavier, deformed nuclei-where most K-isomers are found-has predominantly relied on deformed mean-field approximations [76]. These models employ the concept of spontaneous symmetry breaking, where angular momentum, a crucial quantum number for describing nuclear states, is not conserved in those calculations. Over the years, considerable efforts have been directed towards advancing beyond mean-field descriptions to develop shell models where all excited states are exact eigenstates of angular momentum. It has been emphasized that the angular momentum projection technique is an essential quantum mechanical tool, with the Projected Shell Model (PSM) [77] emerging as a practical model specifically tailored for the study of K-isomers.

Thus, for the microscopic study of nuclear isomeric states in general and the NEEC process in particular, two distinct types of shell models are applicable, sharing the same conceptual framework but differing in their implementation. The first one is the familiar Conventional Shell Model (CSM) that utilizes a spherical basis. The CSM calculation process is conceptually straightforward: it involves constructing a many-body configuration basis, selecting an appropriate Hamiltonian for this basis, and performing numerical diagonalization [78, 79]. Ideally, such calculations yield a comprehensive spectrum of excitations, including low-energy collective states, isomers, and normal states. In practice, however, employing such a CSM to study arbitrarily heavy, deformed nuclei is impractical due to the huge dimensionality of the configuration space and related computational challenges. Even with current computational capabilities, standard CSM calculations are only feasible up to the mass-70 region, where the dimension of the configuration space can approach one billion. For heavier mass regions, general application of the CSM is untenable, and only a few selective calculations are possible for nuclei near closed shells.

In contrast, the second type, the PSM, presents an unconventional approach [77] that significantly diverges from the CSM in both its implementation and the targeted nuclei. The PSM utilizes angular momentum projection, an effective method for truncating the shell model space that would otherwise be unmanageably large [77]. This methodology, pioneered by Hara and Sun in their early work [80], has undergone significant evolution over the years and has been successfully employed in the nuclear spectroscopy of a wide range of isotopes on the nuclear chart [81, 82]. The representative calculations range from light [83] to heavy nuclei [84], extending even to the superheavy mass region [85–87], thereby providing insights into the anticipated superheavy island of stability. Moreover, the PSM has also been utilized in studies of nuclei exhibiting normal and super deformations [86, 87], and has advanced studies on exotic nuclear shapes, including the coexistence of reflection asymmetric and symmetric shapes, as extensively detailed in Ref. [88].

Recently, the PSM has been noticeably expanded to include studies of nuclear level density [89], marking a milestone where shell-model calculations have addressed nuclear levels on the order of 10^6 per MeV for the first time. Within the PSM framework, it is now feasible to simultaneously explore the properties of nuclear isomers and their associated triggering levels. This expansion may have far-reaching implications for the study of isomers in nuclear astrophysics, particularly in scenarios encountered in nucleosynthesis simulations, which involve the transmutation of nuclei via nuclear reactions and decays in thermally excited environments. In the absence of sufficient structural information of excited nuclear states, current nucleosynthesis calculations typically adopt one of these two approaches to approximate nuclear transmutation rates [90]. The simpler approach neglects excited states, focusing solely on the ground state properties of nuclei, as exemplified by discussions on neutrino luminosity via the Urca process [91, 92]. Alternatively, some models assume a thermal-equilibrium population of excited states, with each state contributing to the overall rate of transmutation based on its thermal population probability [93]. However, as demonstrated by Misch *et al*. [59], depending on the specific astrophysical environment, nuclear isomers may challenge the validity of these conventional approaches. Notably, Wang *et al*. provided initial examples [94] demonstrating that the manifestation of isomer effects through the NEEC process is viable and suggesting further investigation in appropriate astrophysical environments.

IV. NEEC IN LASER-INDUCED PLASMAS

The interaction between photons and matter remains a cornerstone of modern physics. The development of

advanced laser technologies, particularly Chirped Pulse Amplification (CPA) [95], has facilitated the creation of environments characterized by ultra-intense and ultra-short electromagnetic fields. When subjected to such fields, target atoms undergo ionization, leading to the formation of plasmas. These plasmas possess electromagnetic fields significantly stronger than those produced by traditional magnetic systems. Within these environments, electrons and ions could be accelerated followed by a series of atomic and nuclear interactions [96–98]. The plasmas generated are capable of achieving extremely high temperatures and densities if needed, which trigger a complex sequence of nuclear reactions, including excitation, transformation, and decay of nuclei. Intense laser-matter interaction thus produces plasmas containing free electrons and various ionic states [7, 19, 71, 99–103].

A. Laser-induced plasma

The invention of the laser in 1960 represented a groundbreaking development, marking the first instance of coherent control over light. This milestone catalyzed rapid advancements in laser technology, notably in the compression of laser pulse durations and the corresponding increase in peak intensities. The proposal and realization of CPA technology significantly advanced these developments, bringing laser pulse durations into the femtosecond and even attosecond regimes, while dramatically enhancing laser intensities [95]. By 2023, three scientists were awarded the Nobel Prize for their contributions to attosecond pulse technology [104–106], underscoring the profound impact of this advancement. In contemporary settings, femtosecond laser pulses can achieve focused intensities as high as 10^{22} W/cm^2 in laboratory environments [107–109]. At such high intensities, the oscillating electric field of the laser far surpasses the internal electric field of atoms, quickly ionizing them into a plasma state. Consequently, the study of laser-plasma interactions has emerged as one of the most active and dynamic areas within the field of plasma physics [110].

The acceleration of electrons and ions driven by laser-plasma interactions provides an ideal experimental platform for investigating photon-nucleus and electron-nucleus reactions. These include photon excitation (PE) [111], coulomb excitation (CE) [112–115], nuclear excitation by electronic transition (NEET) [116–120], electron bridge (EB) [12], photonuclear reaction (γ, n) [7, 121, 122], among others. While both CE and NEET have been experimentally confirmed, NEET typically exhibits a much smaller cross section compared to other processes. The dominant process or processes for nuclear excitation depend critically on specific laser parameters and plasma conditions [99, 123]. Therefore, meticulous calculations, simulations, and experimental investigations are necessary to ascertain whether NEEC or other competing nuclear excitation mechanisms predominate under particular experimental conditions.

B. Laser-ablated plasma

Laser ablation on a solid surface provides a relatively convenient method for generating plasma. The temperature and density of the electrons within this plasma are highly sensitive to both position and time. By combining rough estimates of plasma density and temperature with the cross sections of each relevant nuclear and electronic process, it is possible to approximate the rates of NEEC, NEET, Nuclear Excitation by Inelastic Electron Scattering (NEIES), DR, and RR, which can be estimated [22, 23, 102].

Subsequent studies have refined the determination of plasma conditions by simulating plasma dynamics from their generation to diffusion. J. Gunst *et al.* investigated the NEEC processes in a cold dense plasma environment induced by X-ray Free Electron Laser (XFEL) pulses irradiating on a ^{93m}Mo target [124]. Y. Wu *et al.* investigated the NEEC processes in a femtosecond laser-ablated plasma utilizing a comparable target [72, 125]. Variations in laser parameters lead to plasmas with differing temperatures and densities, which these studies have leveraged to identify optimal experimental setups for observing the NEEC process. In the studies conducted by these researchers, it was emphasized that to effectively induce NEEC events while simultaneously minimizing background noise contributions from processes such as RR and photon excitation, the plasma temperature and density must be maintained at relatively low levels. For instance, laser intensities on the order of 10^{14} to 10^{16} W/cm^2 with energy ranges between 10 mJ and 100 mJ are employed to generate plasma, resulting in a cold plasma where the thermal photon flux is insufficient to induce photon excitation of the nucleus and suppressing the occurrence of NEIES process [72, 126, 127]. Concurrently, the nuclear energy gap should be appropriately low, on the order of several keV, which aligns with the region of the cold plasma that corresponds to the highest density of electron energies. Examples include the 1.565 keV transition in ^{201}Hg, 1.642 keV transition in ^{193}Pt, 2.329 keV transition in ^{205}Pb, 4.821 keV transition in ^{151}Sm, among others, as listed in Ref. [128].

Additionally, in cases where secondary X-rays are generated via inner-shell processes, like noted in Ref. [72], it is crucial to ensure that the plasma density must remain sufficiently low to maintain the stability of inner-shell vacancies, as higher densities would lead to rapid depletion of these vacancies due to RR processes.

P. V. Borisyuk *et al.* conducted an experiment focused on the isomeric excitation of ^{229}Th utilizing a Nd:YAG laser to ablate a Th:SiO_2 target, which contains 6.8% of ^{229}Th [19]. They measured the energy levels and half-life of the generated ^{229}Th isomer, based on their theoretical calculations, it was indicated that the nuclear excitation was induced by the NEEC process. However, the study did not provide detailed analyses to rule out other nuclear-excitation mechanisms, leaving it unclear whether NEEC was indeed the dominant mechanism in this scenario.

C. Laser-heated cluster

The interaction between intense laser pulses and atom clusters offers a unique plasma environment that is well-suited for verifying NEEC [129]. J. Qi *et al.* have proposed a method using laser-cluster interaction to excite ^{229}Th from its ground state to its isomeric state [127]. Their calculations indicate that the isomeric excitation is primarily driven by NEEC and NEIES. By adjusting the laser intensity, it is possible to continuously tune between NEEC and NEIES, providing an approach to confirm the NEEC.

Laser-heated clusters, although nanometer-sized plasmas, exhibit distinct characteristics different from those of ablation plasma plumes. Firstly, cluster nanoplasmas possess simpler plasma characteristics and dynamics, allowing for more effective characterization. Secondly, they exhibit significantly higher electron densities, which accentuate the importance of NEEC and NEIES over other mechanisms. To further isolate NEEC, specific laser intensities can be employed to emphasize NEEC while minimizing the contribution from NEIES. Recently, J. Qi *et al.* demonstrated that the interaction between intense laser pulses and ^{235}U clusters provides an ideal system where the NEEC process account for over 99.9% of the nuclear isomeric excitation [126].

D. Pros and cons of using laser-ablated plasma

Here, we outline some advantages and disadvantages of verifying NEEC using laser-generated plasmas. The advantages may include:

(i) Laser-generated plasmas provide a relatively well-controlled experimental environment where the plasma parameters like temperature, density, and composition can be precisely adjusted and quantitatively measured, facilitating systematic investigations of the NEEC under controlled environmental conditions.

(ii) The ability of laser-generated plasmas to achieve certain temperatures and densities increases the likelihood of NEEC occurrences, providing an suitable setting for the observation and study of this phenomenon.

(iii) Laser-generated plasma experiments enable the exploration of a wide energy range relevant to the NEEC. This capability allows for the investigation of various nuclear systems and energy regimes (e.g., 8 eV for ^{229}Th, 76 eV for ^{235}U, 4.8 keV for ^{93}Mo) by adjusting laser parameters.

The disadvantages of employing laser-generated plasmas for investigating NEEC include:

(i) The short lifespan of laser-generated plasmas, due to rapid cooling and expansion, restricts the temporal window available for NEEC occurrences, potentially limiting experimental observation and analysis of the process.

(ii) Laser-generated plasmas allow for multiple nuclear excitation mechanisms, such as NEEC, NEIES, NEET, and optical excitations. For instance, in cluster nanoplasmas, nuclear excitation predominantly arises from NEEC and NEIES, whereas in plasmas generated by more intense lasers, NEET may predominate. Therefore, detailed calculations are imperative to determine optimal laser parameters to emphasize NEEC over competing processes.

(iii) Interactions within a laser-plasma environment can introduce additional effects like electron heating, ionization, and charge screening, each of which can influence nuclear excitation processes. Accurate simulating and accounting for these effects are necessary to approximate the actual conditions within the plasma.

V. NEEC STUDIES WITH VORTEX BEAMS

Vortex light beams (Fig. 3), first proposed in the 1990s [42], represent a transformative development in photonics. These beams are characterized by photons that carry not only intrinsic spin angular momentum but also orbital angular momenta (OAM). The inclusion of intrinsic OAM introduces a new degree of freedom, distinguishing vortex states from traditional plane-wave states and inspiring extensive exploration of novel phenomena in atomic and nuclear physics. For instance, the theoretical studies on the photodisintegration of deuterons using twisted photons have been discussed in Ref. [130, 131]. These studies examine the dependence of the photodisintegration cross section on the impact parameter b — the distance between the target nucleus and the vortex beam axis. The studies also identify an increased threshold energy required for the reaction, along with interesting features of selection rules for small impact parameters. Similarly, hadron excitation induced by vortex photons has been analyzed in Ref. [132]. More recently, theoretical studies on giant multipole resonances in nuclei induced by vortex γ-photons have been presented in Ref. [133, 134]. These investigations highlight the potential for manipulating the excitation of giant multipole resonances by vortex γ-photons, facilitating transitions that are otherwise forbidden or enabling quasi-pure transitions, provided the nucleus is precisely aligned with the vortex beam axis [133].

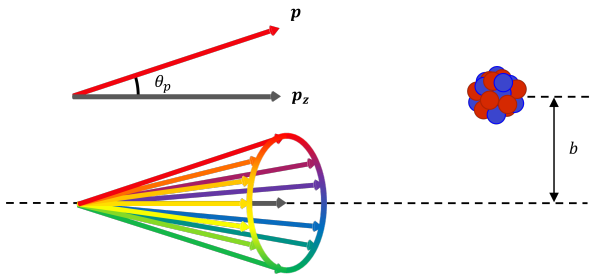

Fig. 3. Composition of a vortex beam: A vortex beam is formed by the coherent superposition of plane waves arranged in a conical configuration. This arrangement gives rise to a helical phase structure and imparts orbital angular momentum (OAM) to the beam. θ_p is the top angle of the cone, while b represents the impact parameter, defined as the perpendicular distance from the beam axis to the target.

The recent advancements in fabricating phase masks with nanometer-level precision have enabled unprecedented

control over the coherent superposition of matter waves, facilitating the generation of vortex beams with chiral wave function spatial profiles that carry OAM [135–139]. By imparting chirality to massive particles, vortex beams have been proposed as novel tools for studying [39–41, 44, 140] and even manipulating [138, 141–143] the structural properties of neutrons, protons, ions, and their associated particle and nuclear processes. Electron vortex beams, among the most extensively studied massive-particle vortex beams, have been experimentally realized using various techniques, such as holographic gratings, phase plates, magnetic monopole fields, or chiral plasmonic near fields [39–41, 44, 135–137]. These beams have achieved angular momenta as high as $1000\hbar$, showcasing their potential for advanced applications.

The potential of vortex electrons to advance nuclear physics has been extensively extensively discussed in Refs. [36, 40, 41, 143]. In particular, the possibility of the manipulation of nuclear excitation via vortex electrons has been studied theoretically in detail, in the context of the NEEC [36].

The NEEC cross section with a vortex electron beam is expressed as [36]

$$\sigma(E) = \frac{4\pi^2}{pJ_z} Y_n \mathcal{L}(\varepsilon - \varepsilon_0), \tag{9}$$

where p is the momentum of the electron, J_z denotes the total incident current, and Y_n is determined through the mapping of the vortex beam onto the partial wave expansion of the continuum electron wave function,

$$\begin{aligned} Y_n &= \frac{b^2}{4\pi} \int_0^{2\pi} \int_0^{2\pi} \frac{d\alpha_p}{2\pi} \frac{d\alpha_k}{2\pi} e^{im(\alpha_p - \alpha_k)} \mathcal{Y}(\mathbf{p}, \mathbf{k}) \\ &\quad \times {}_0F_1(2; u), \end{aligned} \tag{10}$$

with the condition $|\mathbf{p}_\perp| = |\mathbf{k}_\perp| = \zeta$, α_p and α_k being the polar angles of the momentum components, spanning the interval $[0, 2\pi)$, and m denotes the electron orbital angular momentum. The notation ${}_0F_1$ stands for the confluent hypergeometric limit function, and $u = -b^2\zeta^2[1 - \cos(\alpha_k - \alpha_p)]/2$. For a nuclear transition of multipolarity λL, we have

$$\begin{aligned} \mathcal{Y}(\mathbf{p}, \mathbf{k}) &= \frac{16\pi^3(2J_g + 1)}{(2J_i + 1)(2L + 1)^2} \\ &\quad \times B\uparrow(\lambda L)\rho_i \sum_{\kappa, m_l} \frac{\mathcal{Y}_b}{2l + 1} Y^*_{lm_l}(\theta_k, \phi_k) \\ &\quad \times Y_{lm_l}(\theta_p, \phi_p), \end{aligned} \tag{11}$$

where J_i and J_g are the angular momenta of the initial and final electron configuration of the ion, respectively. The term Y_{lm_l} denotes the spherical harmonics characterized by quantum numbers l and m_l, with $\theta_p(\theta_k)$ and $\phi_p(\phi_k)$ being the polar and azimuthal angles of the electron momentum $\mathbf{p}(\mathbf{k})$ in the spherical coordinate system of the ion. Details of the integrals $\mathcal{Y}_b$ can be found in the supplementary material of Ref. [36].

The recombination orbital of the electron and the nuclear transition multipolarity determine selection rules that govern which angular momentum components of the incoming electron participate in the NEEC process. For plane-wave electrons, the wave function has a fixed partial wave expansion across all multipoles. However, vortex electrons can be intentionally shaped to enhance NEEC efficiency [36]. By analyzing isomer depletion in ^{93m}Mo and ^{152m}Eu, representative of E2 and M1 nuclear transitions, respectively. Ref. [36] demonstrates that vortex electrons with a suitable opening angle and quantum number for the orbital angular momentum, and precise control of the distance between the ion and the electron vortex axis, could significantly alter the isomer depletion rate. These results highlight new possibilities for the dynamical control of isomer depletion and other nuclear processes.

It is important to emphasize that the remarkable features observed in nuclear processes involving vortex photons and electrons rely on highly precise positioning of the nucleus relative to the vortex axis, at a scale comparable to the photon wavelength or the inverse transverse momentum of the vortex particle. This behavior has also been noted in studies of vortex photon interactions with atomic systems [43, 44, 144–147]. However, the typical energy scale of nuclear processes, which ranges from keV to several MeV, makes achieving such precision a significant experimental challenge [41]. The use of cold neutron vortex beams may reduce these experimental challenges allowing for the exploration of the intriguing features of vortex particles in nuclear processes [41, 130, 148, 149]. Nonetheless, further research is required to develop methods that relax these stringent conditions while still enabling the observation of these features, especially in the context of the NEEC process. Advancements in this area would be crucial for applications of vortex particles in the manipulation of nuclear processes via the coupling of the nuclear and electronic degrees of freedom.

VI. NEEC STUDIES BASED ON ACCELERATORS

Another approach to study NEEC in laboratory settings involves the use of accelerators, where high-energy beams of highly charged ions are generated.

A. By Using a Storage Ring

In a cooling storage ring, as illustrated in Fig. 4, a cooling electron beam is employed for the ion beam stability. This configuration facilitates electron-ion interaction experiments, which are anticipated to enable observation of the NEEC process. And a heavy ion storage ring provides an ideal experimental environment, in which relatively long-lived isomers interact with electron beams under controlled conditions, analogous to those in DR experiments [150–152].

A. Palffy *et al.* proposed an experimental method for spatially separating photon emissions based on the differing time scales of RR and NEEC processes, while also providing theoretical insights for enhancing the resonance strength of NEEC by introducing fast electronic X-ray decay [33]. In

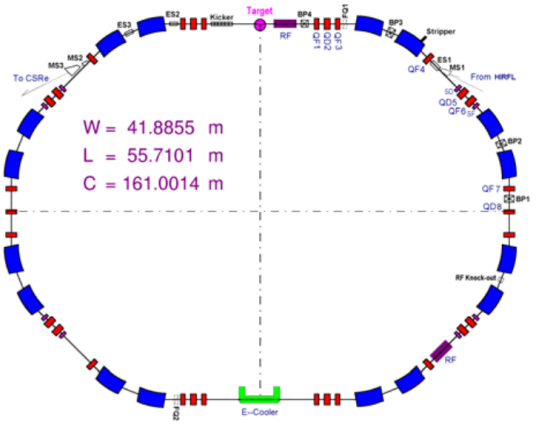

Fig. 4. The layout of the main cooler storage rings (CSRm) at Institute of Modern Physics, Lanzhou, China [153].

this approach, the RR process emits a photon within 10^{-15} s, whereas the NEEC process emits the photon after the excited nucleus with time scale of ns $\sim \mu$s. This temporal separation enables relatively pure confirmation of NEEC events through the detection of delayed photons.

A primary challenge in implementing this method lies in efficiently capturing the excited isomers. Constructing a detector that encompasses the full circumference to capture all emitted photons would be prohibitively expensive. Consequently, it is crucial to develop cost-effective techniques, such as coincidence detection, to enhance the efficiency of capturing these rare events [154]. As shown in Fig. 5, in the description by Yang et al., the NEEC process occurs within the interaction zone, where the circulating ion beam in the CSR interacts with an electron beam originally employed for beam stabilization. A photon detector array is positioned around the interaction zone, while ions, whose charge states are altered due to the occurrence of NEEC or RR processes, are subsequently collected by a particle detector. The NEEC and RR events can be distinguished from each other by the emission time.

Adding another electron beam into storage rings, such as the HIAF [155], holds significant promise for advancing NEEC experimental studies. This approach enables more precise and efficient detection methodologies, significantly expanding the range of isomers available for investigation compared to laser-induced plasma systems. The tunable energy of the electron beam offers enhanced control over resonance conditions, allowing access to a broader spectrum of nuclear energy levels.

B. By Using Ion Beams

When an ion beam is directed at a solid target, the ions traverse the material, undergoing continuous changes in direction and energy. Simultaneously, their states of excitation and ionization may vary due to processes such as electron capture or loss [156–159]. Typically, as the

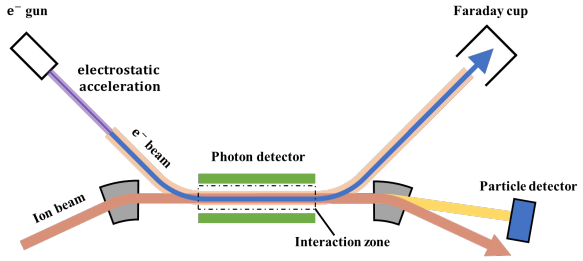

Fig. 5. Proposed experimental layout for NEEC detection employing a storage ring.

velocity of the ions decreases, their average charge state also diminishes. This variation depends significantly on the properties of the target material. During the stopping process, NEEC channels progressively close, beginning with the outer orbitals and moving inward, as shown in Fig.6. For a given orbital, the resonance condition on energy is satisfied at a specific point during the stopping process. If the orbital is not firmly occupied, the corresponding NEEC channel can be activated during the stopping.

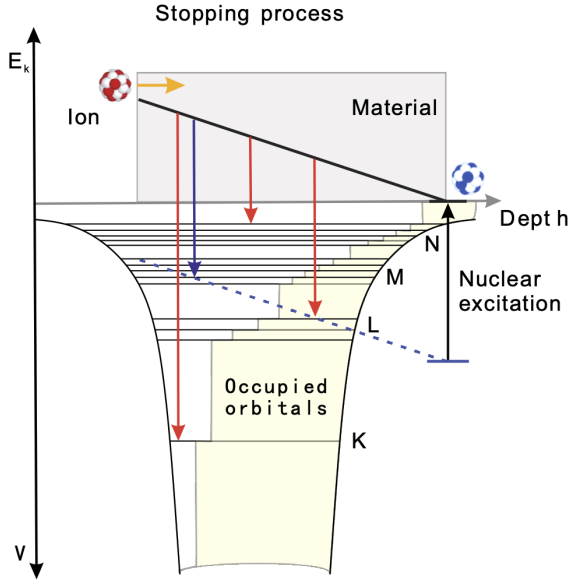

Fig. 6. Schematic diagram of nuclear excitation by electron capture in the ion-stopping process. E_k is the kinetic energy of a free electron in the centroid reference frame of the ion, while V denotes the potential energy of the electron orbitals.

The number of active NEEC channels depends on the energy gap between the isomeric state and the triggering state. Therefore, the NEEC probability can vary significantly among different isomers. Several isomers have been proposed as candidates for experimental measurement based on theoretical predictions. Among them, ^{93m}Mo has attracted special attention due to its favorable properties. This isomer has an excitation energy of 2425 keV, a half life of 6.85 h and a spin and parity of $21/2^+$, as shown in Fig. 7a. A triggering

state with $17/2^+$ lies just 4.8 keV above the isomeric state and has a half-life of 3.5 ns.

The first experimental observation of NEEC was reported by Chiara *et al.* with a probability of 0.010(3) for ^{93m}Mo ions interacting with a carbon foil [17]. The measurements were conducted at the ATLAS facility at Argonne National Laboratory, utilizing the Gammasphere array to detect γ-rays, as shown in Fig.7b. In the experiment, ^{93m}Mo ions were produced at the ^{7}Li target bombarded by a ^{90}Zr beam with a beam energy of 840 MeV, and then implanted in a carbon foil located 3 mm away from the primary target, and finally stopped in the lead backing. The NEEC process was hypothesized to occur within the carbon foil, leading to coincidence detection of γ-rays above the isomeric state and those below the triggering state. The γ-rays from states above the isomeric level exhibited Doppler shifts due to the ion's motion, while those below the triggering state did not, as the ions stopped in the carbon and lead layers within a few picoseconds—a duration much shorter than the half-life of the triggering state.

From a great number of triple or higher-fold coincidence events, the coincidence between the 268-keV transition depopulating the triggering state and the transitions above the $21/2^+$ isomer was extracted to be valid. Based on this, a depletion probability of 0.010(3) was deduced. However, subsequent theoretical studies were unable to reproduce such a large probability, instead predicting a much smaller value of approximately 10^{-11} [31].

Later, it was noted that the handling of background in this experiment might have been overly idealized, potentially leading to an overestimation of the extracted NEEC probability. In a reply, Chiara *et al.* argued that the random coincidence could contribute to only about 0.0008 to the reported probability and the possible contamination in the reported spectra could be explained with some unpublished information [160].

To address the controversy surrounding the NEEC probability, another independent experiment was carried out at the Heavy Ion Research Facility in Lanzhou (HIRFL), as shown in Fig.7c [18]. In this experiment, an ^{86}Kr beam with an energy of 559 MeV was directed onto a carbon target positioned at T0 of the secondary Radioactive Ion Beam Line in Lanzhou (RIBLL). The resulting ^{93m}Mo ions were transported by RIBLL to the detection station located at T2, and stopped in a plastic scintillator. NEEC of ^{93m}Mo ions was was anticipated to occur during their deceleration in a 20μm-thick carbon foil located in front of the plastic scintillator. γ-rays emitted from the NEEC process and subsequent isomeric transitions were detected by five Compton-suppressed High-Purity Germanium (HPGe) detectors surrounding the plastic scintillator, while the prompt γ-rays from the primary fusion-evaporation reactions were emitted at T0 and do not contribute to the background of the measurement. The NEEC of ^{93m}Mo was not observed in this experiment, with an upper limit of the NEEC probability of 2×10^{-5}.

However, the recoiling energy in the latter experiment is considerably lower, and the stopping materials used differ between the two experiments. As a result, the debate persists on both experimental and theoretical fronts. Further experiments will be required to provide conclusive evidence and resolve the discrepancies.

C. By Using Electron Beams

Since NEEC is a resonant process, the selection and preparation of appropriate energy levels and ion charge states are critical for its successful observation. An electron beam ion trap (EBIT) offers an alternative environment for these studies, providing a tunable electron beam and well-confined highly charged ions.

In an EBIT, ions are confined within a narrow spatial region, primarily centered around the electron beam, as illustrated in Fig. 8. The the electron beam density ranges from approximately 10^{10} to 10^{12} cm^{-3}. The equilibrium charge state of the ions can be controlled by adjusting key parameters such as the electron beam energy, the axial magnetic field, and the presence of neutral atoms in the trap region, as detailed in [161].

In Ref. [35], Jon Ringuette conducted simulations of the NEEC process at the TITAN setup to excite ^{129m}Sb ($T_{1/2}$ = 17.7 min) to a state 10-keV higher. However, careful selection of the ion charge state and atomic orbitals is necessary to overcome challenges arising from switching the electron beam from the charge breeding energy to the NEEC resonance energy. In Ref. [20], Y. Wang *et al.* proposed a modified EBIT configuration that features two electron guns with different energy settings: the one is optimized to strip atoms to the high charge states, while the other is tuned to meet the NEEC resonance conditions. In the experimental setups proposed by these researchers, the confirmation of NEEC events is achieved by detecting the emitted photons through an observation window around the drift tubes.

In the experimental setups proposed by these researchers, the confirmation of NEEC events may be achieved by detecting the emitted photons through an observation window around the drift tubes. As noted by Wang et al., differentiation between NEEC events and background signals, particularly from the RR process, primarily relies on their distinct angular distributions. Developing a more comprehensive approach for detection and discrimination, along with further optimization of experimental conditions, remains an active area of investigation.

The NEEC counting rate is significantly influenced by the energy distribution of the electron beam in an EBIT [35]. Additionally, it has been demonstrated that NEEC signals can be effectively distinguished from the RR background only when the experimental conditions, particularly the electron beam, are well defined [27].

VII. SUMMARY

The Nuclear Excitation by Electron Capture (NEEC) process, along with its inverse process, internal conversion,

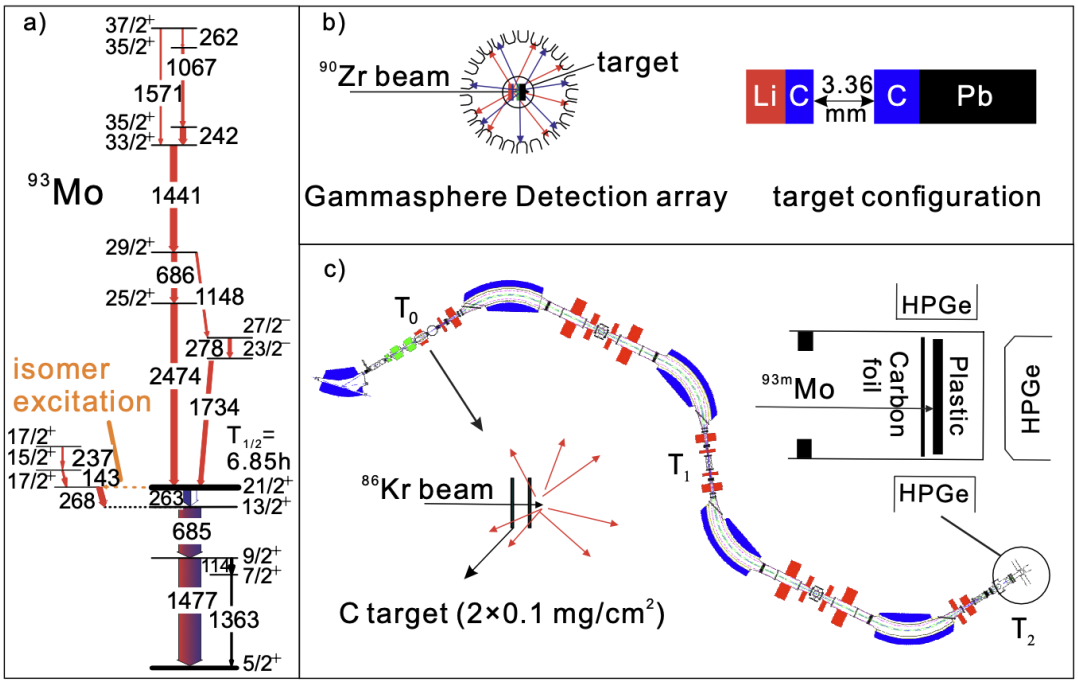

Fig. 7. Structure of ^{93}Mo and the settings of two experiments. a) Level scheme of ^{93}Mo; b) The setting diagram of the experiment carried out at Argonne Laboratory in the United States; c) Schematic diagram of the experiment based on the Heavy Ion Research Facility in Lanzhou.

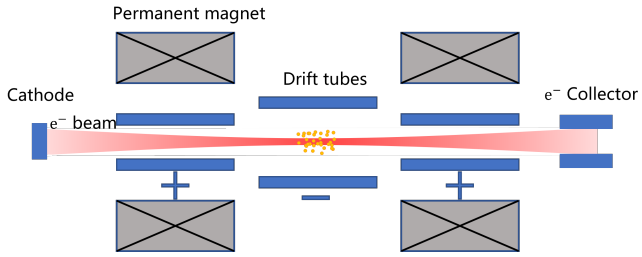

Fig. 8. Setup structure of EBIT, composed of a cathode, permanent magnets, drift tubes, and an electron collector.

represents a unique interaction that simultaneously involves both atomic and nuclear structures. NEEC and IC are closely related to the excitation or de-excitation of nuclear isomeric states, with implications for technological applications and fundamental physics, including nuclear batteries, nuclear clocks, and nucleosynthesis in astrophysical environments.

Since its theoretical proposal in 1976, NEEC has attracted considerable attention from the scientific community. A number of researchers in related fields have suggested that NEEC could play a significant role in astrophysical environments and plasma physics. In astrophysics, NEEC could extend the reaction chains of neutron capture processes, potentially altering the isotopic abundances in stellar and cosmic contexts. In plasma environments, NEEC could influence the population balance of atomic nuclei and their associated isomers.

Nevertheless, despite its theoretical potential, experimental verification of NEEC has remained a formidable challenge. Key challenges include the high background noise inherent to experimental environments, whether in laser-induced plasmas or particle accelerators. In these settings, the NEEC cross section is small compared to other competing electromagnetic interactions, such as Coulomb Excitation and Radiative Recombination, complicating the task of isolating NEEC signals from substantial noise. Consequently, experimental confirmation of NEEC has remained elusive. Efforts to enhance NEEC rates and mitigate background interference continue to be active areas of research.

In the selection of experimental setups and the design of experimental schemes, some researchers, such as J. Gunst, Y. Wu, and J. Qi, have explored optimal laser parameters and plasma properties for NEEC to occur in laser-induced plasmas. They suspected that using low-energy-density lasers on solid targets to generate cold, low-density plasmas can effectively reduce noise and enhance the occurrence and detection of NEEC events. In plasma environments, the detection scheme for NEEC with X-rays tends to focus on nuclei or isomer with low gaps above, typically in the eV to keV range. On the other hand, researchers such as A. Palffy, Chiara, Jon Ringuette, and Y. Wang have focused on demonstrating that precise energy control via electron or ion beams can improve the efficiency of NEEC, thereby reducing the influence of noise. They employ techniques such as storage rings, ion-beam interactions with solids, or electron-beam interactions with plasmas, which significantly expand the range of selectable nuclear energy levels. In particular, if dual electron beams are used in a storage rings or EBIT setup, the efficiency of reactions can be enhanced while maintaining the stability of the ion beam in the storage

ring or the plasmas in EBIT. These methodologies, however, still require further refinement and development in future experimental setups.

Additionally, it should be noted that owing to the inherent properties of nuclear transition selection rules, higher order multipole transitions are typically suppressed, resulting in insufficient reaction cross-sections. X. Wang et al. have introduced vertex beams into the study of NEEC, developing a theoretical framework for their application. Due to the orbital angular momentum (OAM) carried by vortex beams, the traditional selection rules are broken, enabling the occurrence of higher order multipole transitions. The successful generation of high-intensity vertex beams in laboratory environments could thus represent a significant breakthrough, potentially advancing the study of nuclear excitation processes.

Efforts to design experiments that effectively eliminate background noise and enable the discovery of NEEC remain an active area of research. Successfully confirming NEEC would mark a significant breakthrough in our understanding of nuclear processes, paving the way for advancements in both fundamental research and practical applications.

[1] V. Goldanskii, V. Namiot, On the excitation of isomeric nuclear levels by laser radiation through inverse internal electron conversion. Physics Letters B **62**, 393 (1976). doi:10.1016/0370-2693(76)90665-1

[2] S. Dancoff, P. Morrison, The calculation of internal conversion coefficients. Physical Review **55**, 122 (1939). doi:10.1103/PhysRev.55.122

[3] N. Tralli, G. Goertzel, The theory of internal conversion. Physical Review **83**, 399 (1951). doi:10.1103/PhysRev.83.399

[4] E. Church, J. Weneser, Nuclear structure effects in internal conversion. Annual review of nuclear science **10**, 193–234 (1960). doi:10.1146/annurev.ns.10.120160.001205

[5] W. De-jin, C. Ling, Plasma astrophysics and modern plasma cosmology. Chinese Astronomy and Astrophysics **47**, 490–535 (2023). doi:10.1016/j.chinastron.2023.09.003

[6] S. Surti, A.R. Pantel, J.S. Karp, Total body pet: Why, how, what for? IEEE Transactions on Radiation and Plasma Medical Sciences **4**, 283–292 (2020).

[7] H.Y. Lan, D. Wu, J.X. Liu et al., Photonuclear production of nuclear isomers using bremsstrahlung induced by laser-wakefield electrons. Nuclear Science and Techniques **34**, 74 (2023). doi:10.1007/s41365-023-01219-x

[8] O. Artun, A study of nuclear structure for ^{244}Cm, ^{241}Am, ^{238}Pu, ^{210}Po, ^{147}Pm, ^{137}Cs, ^{90}Sr and ^{63}Ni nuclei used in nuclear battery. Modern Physics Letters A **32**, 1750117 (2017). doi:10.1142/S0217732317501176

[9] V. Kirischuk, V. Ageev, A. Dovbnya et al., Induced acceleration of the decay of the 31-yr isomer of ^{178m2}Hf using bremsstrahlung radiation. Physics Letters B **750**, 89–94 (2015). doi:10.1016/j.physletb.2015.08.051

[10] F.F. Karpeshin, M.B. Trzhaskovskaya, L.F. Vitushkin, Electron recombination as a way of deexciting the ^{129m}Sb isomer. Bulletin of the Russian Academy of Sciences: Physics **84**, 1207–1209 (2020). doi:10.3103/S1062873820100135

[11] L. Li, Z. Li, C. Wang et al., Scheme for the excitation of thorium-229 nuclei based on electronic bridge excitation. Nuclear Science and Techniques **34**, 24 (2023). doi:10.1007/s41365-023-01169-4

[12] N.Q. Cai, G.Q. Zhang, C.B. Fu et al., Populating ^{229m}Th via two-photon electronic bridge mechanism. Nuclear Science and Techniques **32**, 59 (2021). doi:10.1007/s41365-021-00900-3

[13] M. Prelas, Introduction to Nuclear-Pumped Lasers, (Springer International Publishing, Cham, 2016), pp. 1–61

[14] A. Pálffy, J. Evers, C.H. Keitel, Isomer triggering via nuclear excitation by electron capture. Physical review letters **99**, 172502 (2007). doi:10.1103/PhysRevLett.99.172502

[15] N. Cue, Nuclear excitation by target electron capture. Nuclear Instruments and Methods in Physics Research Section B: Beam Interactions with Materials and Atoms **40**, 25–27 (1989). doi:10.1016/0168-583X(89)90914-2

[16] Z.S. Yuan, J. Kimball, First-principles calculation of the cross sections for nuclear excitation by electron capture of channeled nuclei. Physical Review C **47**, 323 (1993). doi:10.1103/PhysRevC.47.323

[17] C. Chiara, J. Carroll, M. Carpenter et al., Isomer depletion as experimental evidence of nuclear excitation by electron capture. Nature **554**, 216–218 (2018). doi:10.1038/nature25483

[18] S. Guo, B. Ding, X. Zhou et al., Probing ^{93m}Mo isomer depletion with an isomer beam. Physical Review Letters **128**, 242502 (2022). doi:10.1103/PhysRevLett.128.242502

[19] P.V. Borisyuk, E.V. Chubunova, N.N. Kolachevsky et al., Excitation of ^{229}Th nuclei in laser plasma: the energy and half-life of the low-lying isomeric state. . arXiv:1804.00299

[20] Y. Wang, Z. Ma, Y. Yang et al., Feasibility study of nuclear excitation by electron capture using an electron beam ion trap. Frontiers in Physics **11**,. doi:10.3389/fphy.2023.1203401

[21] Y.k. Ho, Z.s. Yuan, B.h. Zhang et al., Self-consistent description for x-ray, auger electron, and nuclear excitation by electron transition processes. Physical Review C **48**, 2277 (1993). doi:10.1103/PhysRevC.48.2277

[22] M. Harston, J. Chemin, Mechanisms of nuclear excitation in plasmas. Physical Review C **59**, 2462 (1999). doi:10.1103/PhysRevC.59.2462

[23] G. Gosselin, P. Morel, Enhanced nuclear level decay in hot dense plasmas. Physical Review C **70**, 064603 (2004). doi:10.1103/PhysRevC.70.064603

[24] A. Pálffy, W. Scheid, Z. Harman, Theory of nuclear excitation by electron capture for heavy ions. Physical Review A **73**, 012715 (2006). doi:10.1103/PhysRevA.73.012715

[25] Y. Hahn, in Advances in atomic and molecular physics, Theory of dielectronic recombination. Vol. 21, (Elsevier, 1985), pp. 123–196

[26] A. Ichihara, J. Eichler, Cross sections for radiative recombination and the photoelectric effect in the K, L, and M shells of one-electron systems with $1 \leq z \leq 112$ calculated within an exact relativistic description. Atomic Data and Nuclear Data Tables **74**, 1–121 (2000). doi:10.1006/adnd.1999.0825

[27] A. Pálffy, Z. Harman, W. Scheid, Quantum interference between nuclear excitation by electron capture and radiative recombination. Physical Review A **75**, 012709 (2007).

doi:10.1103/PhysRevA.75.012709
[28] A. Pálffy, Nuclear effects in atomic transitions. Contemporary Physics **51**, 471–496 (2010). doi:10.1080/00107514.2010.493325
[29] S. Karamian, J. Carroll, Possible depletion of isomers in perturbed atomic environments. Laser physics **20**, 977–984 (2010). doi:10.1134/S1054660X10090355
[30] S. Karamian, J. Carroll, Calculated yield of isomer depletion due to neec for ^{93m}Mo recoils. Physics of Atomic Nuclei **75**, 1362–1367 (2012). doi:10.1134/S1063778812110117
[31] Y. Wu, C.H. Keitel, A. Pálffy, Mo 93 m isomer depletion via beam-based nuclear excitation by electron capture. Physical review letters **122**, 212501 (2019). doi:10.1103/PhysRevLett.122.212501
[32] J. Rzadkiewicz, M. Polasik, K. Słabkowska et al., Novel approach to mo 93 m isomer depletion: Nuclear excitation by electron capture in resonant transfer process. Physical Review Letters **127**, 042501 (2021). doi:10.1103/PhysRevLett.127.042501
[33] A. Pálffy, Z. Harman, C. Kozhuharov et al., Nuclear excitation by electron capture followed by fast x-ray emission. Physics Letters B **661**, 330–334 (2008). doi:10.1016/j.physletb.2008.02.027
[34] S. Gargiulo, I. Madan, F. Carbone, Nuclear excitation by electron capture in excited ions. Phys. Rev. Lett. **128**, 212502 (2022). doi:10.1103/PhysRevLett.128.212502
[35] J. Ringuette, Towards nuclear excitation via electron capture in an electron beam ion trap. Ph.D. thesis, Colorado School of Mines (2022)
[36] Y. Wu, S. Gargiulo, F. Carbone et al., Dynamical control of nuclear isomer depletion via electron vortex beams. Physical Review Letters **128**, 162501 (2022). doi:10.1103/PhysRevLett.128.162501
[37] Y. Shen, X. Wang, Z. Xie et al., Optical vortices 30 years on: Oam manipulation from topological charge to multiple singularities. Light: Science & Applications **8**, 90 (2019). doi:10.1038/s41377-019-0194-2
[38] K.Y. Bliokh, F. Nori, Transverse and longitudinal angular momenta of light. Physics Reports **592**, 1–38 (2015). doi:.1016/j.physrep.2015.06.003
[39] S. Lloyd, M. Babiker, G. Thirunavukkarasu et al., Electron vortices: Beams with orbital angular momentum. Reviews of Modern Physics **89**, 035004 (2017). doi:10.1103/RevModPhys.89.035004
[40] K.Y. Bliokh, I.P. Ivanov, G. Guzzinati et al., Theory and applications of free-electron vortex states. Physics Reports **690**, 1–70 (2017). doi:10.1016/j.physrep.2017.05.006
[41] I.P. Ivanov, Promises and challenges of high-energy vortex states collisions. Progress in Particle and Nuclear Physics **127**, 103987 (2022). doi:10.1016/j.ppnp.2022.103987
[42] L. Allen, M.W. Beijersbergen, R. Spreeuw et al., Orbital angular momentum of light and the transformation of laguerre gaussian laser modes. Physical review A **45**, 8185 (1992). doi:10.1103/PhysRevA.45.8185
[43] C.T. Schmiegelow, J. Schulz, H. Kaufmann et al., Transfer of optical orbital angular momentum to a bound electron. Nature communications **7**, 12998 (2016). doi:10.1038/ncomms12998
[44] R. Lange, N. Huntemann, A. Peshkov et al., Excitation of an electric octupole transition by twisted light. Physical Review Letters **129**, 253901 (2022). doi:10.1103/PhysRevLett.129.253901
[45] K. Alder, A. Bohr, T. Huus et al., Study of nuclear structure by electromagnetic excitation with accelerated ions. Rev. Mod. Phys. **28**, 432–542 (1956). doi:10.1103/RevModPhys.28.432
[46] A. Gagyi-Palffy, Theory of nuclear excitation by electron capture for heavy ions. Ph.D. thesis, Justus Liebig University Giessen (2006)
[47] S. Helmrich, K. Spenneberg, A. Pálffy, Coupling highly excited nuclei to the atomic shell in dense astrophysical plasmas. Phys. Rev. C **90**, 015802 (2014). doi:10.1103/PhysRevC.90.015802
[48] A. Aprahamian, Y. Sun, Long live isomer research. Nature Physics **1**, 81–82 (2005). doi:10.1038/nphys150
[49] S. Garg, B. Maheshwari, B. Singh et al., Atlas of nuclear isomers-second edition. Atomic Data and Nuclear Data Tables **150**, 101546 (2023). doi:10.1016/j.adt.2022.101546
[50] Y. Sun, Excited nuclear states and k-isomers in the projected shell model. The European Physical Journal Special Topics **233**, 1037–1045 (2024). doi:10.1140/epjs/s11734-024-01095-5
[51] J.J. Carroll, Nuclear structure and the search for induced energy release from isomers. Nuclear Instruments and Methods in Physics Research Section B: Beam Interactions with Materials and Atoms **261**, 960–964 (2007).
[52] J.J. Carroll, Nuclear metastables for energy and power: status and challenges. Innovations in Army Energy and Power Materials Technologies **36**, 289 (2018).
[53] J.J. Carroll, C.J. Chiara, Isomer depletion. The European Physical Journal Special Topics **233**, 1151–1160 (2024). doi:10.1140/epjs/s11734-024-01149-8
[54] Z. Ma, C. Fu, W. He et al., Manipulation of nuclear isomers with lasers: mechanisms and prospects. Science Bulletin **67**, 1526–1529 (2022). doi:10.1016/j.scib.2022.06.020
[55] C.M. Baglin, Nuclear data sheets for A $=$ $81.NuclearDataSheets\mathbf{109}, 2257 - -2437(2008).doi : 10.1016/j.nds.2008.09.001$
[56] C. Collins, F. Davanloo, M. Iosif et al., Accelerated emission of gamma rays from the 31-yr isomer of ^{178}Hf induced by x-ray irradiation. Physical review letters **82**, 695 (1999). doi:10.1103/PhysRevLett.82.695
[57] I. Ahmad, J.C. Banar, J.A. Becker et al., Search for x-ray induced decay of the 31-yr isomer of ^{178}Hf using synchrotron radiation. Phys. Rev. C **71**, 024311 (2005). doi:10.1103/PhysRevC.71.024311
[58] J. Carroll, S. Karamian, R. Propri et al., Search for low-energy induced depletion of ^{178}Hf^{m2} at the spring-8 synchrotron. Physics Letters B **679**, 203–208 (2009). doi:10.1016/j.physletb.2009.07.025
[59] G.W. Misch, S.K. Ghorui, P. Banerjee et al., Astromers: nuclear isomers in astrophysics. The Astrophysical Journal Supplement Series **252**, 2 (2020). doi:10.3847/1538-4365/abc41d
[60] R.H. Cyburt, B.D. Fields, K.A. Olive et al., Big bang nucleosynthesis: Present status. Rev. Mod. Phys. **88**, 015004 (2016). doi:10.1103/RevModPhys.88.015004
[61] G.W. Misch, M.R. Mumpower, Astromers: status and prospects. The European Physical Journal Special Topics **233**, 1075–1099 (2024). doi:10.1140/epjs/s11734-024-01136-z
[62] E.P.B.A.T. Masa-aki Hashimoto, Riou Nakamura, K. Arai, Big-Bang Nucleosynthesis: Thermonuclear History in the Early Universe, 1st Edition, (Springer Singapore, 152 Beach Road, #21-01/04 Gateway East, Singapore 189721, Singapore, 2018). doi:10.1007/978-981-13-2935-7
[63] A. Arcones, F.K. Thielemann, Origin of the elements. The Astronomy and Astrophysics Review **31**, 1 (2022). doi:10.1007/s00159-022-00146-x

[64] T.P. Walker, G. Steigman, D.N. Schramm et al., Primordial Nucleosynthesis Redux. Astrophys. J. **376**, 51 (1991). doi:10.1086/170255

[65] K.A. Olive, G. Steigman, T.P. Walker, Primordial nucleosynthesis: theory and observations. Physics Reports **333-334**, 389–407 (2000). doi:10.1016/S0370-1573(00)00031-4

[66] B.D. Fields, K.A. Olive, Big bang nucleosynthesis. Nuclear Physics A **777**, 208–225 (2006). Special Isseu on Nuclear Astrophysics. doi:10.1016/j.nuclphysa.2004.10.033

[67] G. Gosselin, P. Morel, P. Mohr, Modification of nuclear transitions in stellar plasma by electronic processes: K isomers in ^{176}Lu and ^{180}Ta under s-process conditions. Phys. Rev. C **81**, 055808 (2010). doi:10.1103/PhysRevC.81.055808

[68] S. Helmrich, Nuclear excitation by electron capture in stellar environments. 2011

[69] H. Gan, Nuclear reactions in astrophysical plasmas. Ph.D. thesis, University of Heidelberg (2017)

[70] M. Hasegawa, Y. Sun, S. Tazaki et al., Characteristics of the $21/2^+$ isomer in ^{93}Mo: Toward the possibility of enhanced nuclear isomer decay. Physics Letters B **696**, 197–200 (2011). doi:10.1016/j.physletb.2010.10.065

[71] J. Gunst, Y. Wu, C.H. Keitel et al., Nuclear excitation by electron capture in optical-laser-generated plasmas. Physical Review E **97**, 063205 (2018). doi:10.1103/PhysRevE.97.063205

[72] Y. Wu, C.H. Keitel, A. Pálffy, X-ray-assisted nuclear excitation by electron capture in optical laser-generated plasmas. Physical Review A **100**, 063420 (2019). doi:10.1103/PhysRevA.100.063420

[73] J.W. Negele, The mean-field theory of nuclear structure and dynamics. Rev. Mod. Phys. **54**, 913–1015 (1982). doi:10.1103/RevModPhys.54.913

[74] E. Caurier, G. Martínez-Pinedo, F. Nowacki et al., The shell model as a unified view of nuclear structure. Rev. Mod. Phys. **77**, 427–488 (2005). doi:10.1103/RevModPhys.77.427

[75] T. Otsuka, A. Gade, O. Sorlin et al., Evolution of shell structure in exotic nuclei. Rev. Mod. Phys. **92**, 015002 (2020). doi:10.1103/RevModPhys.92.015002

[76] A.K. Jain, B. Maheshwari, A. Goel, K-Isomers in Deformed Nuclei, (Springer International Publishing, Cham, 2021), pp. 79–99. doi:10.1007/978-3-030-78675-5_5

[77] Y. Sun, Projection techniques to approach the nuclear many-body problem. Physica Scripta **91**, 043005 (2016). doi:10.1088/0031-8949/91/4/043005

[78] Y. Tsunoda, T. Otsuka, Configuration Interaction Approach to Atomic Nuclei: The Shell Model, (Springer Nature Singapore, Singapore, 2020), pp. 1–49. doi:10.1007/978-981-15-8818-1_17-1

[79] N. Shimizu, T. Abe, M. Honma et al., Monte carlo shell model studies with massively parallel supercomputers. Physica Scripta **92**, 063001 (2017). doi:10.1088/1402-4896/aa65e4

[80] K. Hara, Y. Sun, Projected shell model and high-spin spectroscopy. International Journal of Modern Physics E **4**, 637–785 (1995). doi:10.1142/S0218301395000250

[81] Y. Sun et al., High spin spectroscopy with the projected shell model. Physics reports **264**, 375–391 (1996). doi:10.1016/0370-1573(95)00049-6

[82] Y. Sun, K. Hara, Fortran code of the projected shell model: feasible shell model calculations for heavy nuclei. Computer physics communications **104**, 245–258 (1997). doi:10.1016/S0010-4655(97)00064-7

[83] K. Hara, Y. Sun, T. Mizusaki, Backbending mechanism of ^{48}Cr. Physical review letters **83**, 1922 (1999).

[84] Y. Sun, C.L. Wu, K. Bhatt et al., Scissors-mode vibrations and the emergence of su (3) symmetry from the projected deformed mean field. Physical review letters **80**, 672 (1998). doi:10.1103/PhysRevLett.83.1922

[85] R.D. Herzberg, P. Greenlees, P. Butler et al., Nuclear isomers in superheavy elements as stepping stones towards the island of stability. Nature **442**, 896–899 (2006). doi:10.1038/nature05069

[86] Y. Sun, J.y. Zhang, M. Guidry et al., Theoretical constraints for observation of superdeformed bands in the mass-60 region. Physical review letters **83**, 686 (1999). doi:10.1103/PhysRevLett.83.686

[87] Y. Sun, J.y. Zhang, M. Guidry, Systematic description of yrast superdeformed bands in even-even nuclei of the mass-190 region. Physical review letters **78**, 2321 (1997). doi:10.1103/PhysRevLett.78.2321

[88] S. Zhu, E. Wang, J. Hamilton et al., Coexistence of reflection asymmetric and symmetric shapes in ^{144}Ba. Physical Review Letters **124**, 032501 (2020). doi:10.1103/PhysRevLett.124.032501

[89] J. Wang, S. Dutta, L.J. Wang et al., Projected shell model description of nuclear level density: Collective, pair-breaking, and multiquasiparticle regimes in even-even nuclei. Physical Review C **108**, 034309 (2023). doi:10.1103/PhysRevC.108.034309

[90] G.W. Misch, T.M. Sprouse, M.R. Mumpower et al., Sensitivity of neutron-rich nuclear isomer behavior to uncertainties in direct transitions. Symmetry **13**, 1831 (2021). doi:10.3390/sym13101831

[91] H. Schatz, S. Gupta, P. Möller et al., Strong neutrino cooling by cycles of electron capture and β- decay in neutron star crusts. Nature **505**, 62–65 (2014). doi:10.1038/nature12757

[92] A. Deibel, Z. Meisel, H. Schatz et al., Urca cooling pairs in the neutron star ocean and their effect on superbursts. The Astrophysical Journal **831**, 13 (2016). doi:10.3847/0004-637X/831/1/13

[93] G.M. Fuller, W.A. Fowler, M.J. Newman, Stellar weak-interaction rates for sd-shell nuclei. I-nuclear matrix element systematics with application to al-26 and selected nuclei of importance to the supernova problem. The Astrophysical Journal Supplement Series **42**, 447–447 (1980). doi:10.1086/190657

[94] L.J. Wang, L. Tan, Z. Li et al., Urca cooling in neutron star crusts and oceans: Effects of nuclear excitations. Physical Review Letters **127**, 172702 (2021). doi:10.1103/PhysRevLett.127.172702

[95] D. Strickland, G. Mourou, Compression of amplified chirped optical pulses. Optics Communications **56**, 219–221 (1985). doi:10.1016/0030-4018(85)90120-8

[96] S. Eliezer, The interaction of high-power lasers with plasmas. Plasma Physics and Controlled Fusion **45**, 181 (2003). doi:10.1088/0741-3335/45/2/701

[97] H. Daido, M. Nishiuchi, A.S. Pirozhkov, Review of laser-driven ion sources and their applications. Reports on Progress in Physics **75**, 056401 (2012). doi:10.1088/0034-4885/75/5/056401

[98] V. Ospina-Bohórquez, C. Salgado-López, M. Ehret et al., Laser-driven ion and electron acceleration from near-critical density gas targets: Towards high-repetition rate operation in the 1 pw, sub-100 fs laser interaction regime. Phys. Rev. Res. **6**, 023268 (2024). doi:10.1103/PhysRevResearch.6.023268

[99] W. Wang, X. Wang, Quantum theory of isomeric excitation

of ^{229}Th in strong laser fields. Physical Review Research **5**, 043232 (2023). doi:10.1103/PhysRevResearch.5.043232

[100] A. Pálffy, J. Evers, C.H. Keitel, Electric-dipole-forbidden nuclear transitions driven by super-intense laser fields. Phys. Rev. C **77**, 044602 (2008). doi:10.1103/PhysRevC.77.044602

[101] Q. Xiao, J.H. Cheng, Y.Y. Xu et al., α decay in extreme laser fields within a deformed gamow-like model. Nuclear Science and Techniques **35**, 27 (2024). doi:10.1007/s41365-024-01371-y

[102] Y.R. Shou, X.Z. Wu, G.E. Ahn et al., Spatial and spectral measurement of laser-driven protons through radioactivation. Nuclear Science and Techniques **34**,. doi:10.1007/s41365-023-01324-x

[103] Z.C. Li, Y. Yang, Z.W. Cao et al., Effective extraction of photoneutron cross-section distribution using gamma activation and reaction yield ratio method. Nuclear Science and Techniques **34**, 170 (2023). doi:10.1007/s41365-023-01330-z

[104] M. Lewenstein, P. Balcou, M. Ivanov et al., Theory of high-harmonic generation by low-frequency laser fields. Physical Review A **49**, 2117–2132 (1994). Cited by: 3758; All Open Access, Bronze Open Access. doi:10.1103/PhysRevA.49.2117

[105] M. Hentschel, R. Kienberger, C. Spielmann et al., Attosecond metrology. Nature **414**, 509–513 (2001). Cited by: 2739. doi:10.1038/35107000

[106] P. Paul, E. Toma, P. Breger et al., Observation of a train of attosecond pulses from high harmonic generation. Science **292**, 1689–1692 (2001). Cited by: 2422. doi:10.1126/science.1059413

[107] S. Bahk, P. Rousseau, T. Planchon et al., Generation and characterization of the highest laser intensities (10^{22} W/cm^2). Optics letters **29**, 2837—2839 (2004). doi:10.1364/ol.29.002837

[108] V. Chvykov, P. Rousseau, S. Reed et al., Generation of 10^{11} contrast 50 TW laser pulses. Opt. Lett. **31**, 1456–1458 (2006). doi:10.1364/OL.31.001456

[109] V. Yanovsky, V. Chvykov, G. Kalinchenko et al., Ultra-high intensity-300-TW laser at 0.1 Hz repetition rate. Optics Express **16**, 2109–2114 (2008). doi:10.1364/oe.16.002109

[110] H. Takabe, Relativistic Laser and Solid Target Interactions, (Springer International Publishing, Cham, 2020), pp. 239–285. doi:10.1007/978-3-030-49613-5$_7$

[111] C.B. Collins, F. Davanloo, M.C. Iosif et al., Accelerated emission of gamma rays from the 31-yr isomer of ^{178}Hf induced by x-ray irradiation. Phys. Rev. Lett. **82**, 695–698 (1999). doi:10.1103/PhysRevLett.82.695

[112] R. Hofstadter, H. Fechter, J. McIntyre, High-energy electron scattering and nuclear structure determinations. Physical Review **92**, 978 (1953). doi:10.1103/PhysRev.92.978

[113] E. Tkalya, Excitation of ^{229m}Th at inelastic scattering of low energy electrons. Physical Review Letters **124**, 242501 (2020). doi:10.1103/PhysRevLett.124.242501

[114] H. Zhang, W. Wang, X. Wang, Nuclear excitation cross section of ^{229}Th via inelastic electron scattering. Physical Review C **106**, 044604 (2022). doi:10.1103/PhysRevC.106.044604

[115] B. Liu, X. Wang, Isomeric excitation of ^{235}U by inelastic scattering of low-energy electrons. Physical Review C **106**, 064604 (2022). doi:10.1103/PhysRevC.106.064604

[116] M. Morita, Nuclear excitation by electron transition and its application to uranium 235 separation. Progress of Theoretical Physics **49**, 1574–1586 (1973). doi:10.1143/PTP.49.1574

[117] H. Fujioka, K. Ura, Nanosecond stroboscopic electron spectroscopy for observation of nuclear excitation by electron transition (NEET) in ^{197}Au. Japanese Journal of Applied Physics **24**, 1703 (1985). doi:10.1143/JJAP.24.1703

[118] E. Tkalya, Nuclear excitation in atomic transitions (NEET process analysis). Nuclear Physics A **539**, 209–222 (1992). doi:10.1016/0375-9474(92)90267-N

[119] S.a. Kishimoto, Y. Yoda, M. Seto et al., Observation of nuclear excitation by electron transition in ^{197}Au with synchrotron x rays and an avalanche photodiode. Physical Review Letters **85**, 1831 (2000). doi:10.1103/PhysRevLett.85.1831

[120] S. Sakabe, K. Takahashi, M. Hashida et al., Elements and their transitions feasible for NEET. Atomic Data and Nuclear Data Tables **91**, 1–7 (2005). doi:10.1016/j.adt.2005.07.002

[121] W. ting Pan, T. Song, H. yang Lan et al., Photo-excitation production of medically interesting isomers using intense γ-ray source. Applied Radiation and Isotopes **168**, 109534 (2021). doi:10.1016/j.apradiso.2020.109534

[122] G.L. Wang, H.Y. Lan, X.M. Shi et al., A general framework for describing photofission observables of actinides at an average excitation energy below 30 mev *. Chinese Physics C **46**, 084102 (2022). doi:10.1088/1674-1137/ac6abc

[123] H. Zhang, X. Wang, Theory of isomeric excitation of ^{229}Th via electronic processes. Frontiers in Physics **11**, 1166566 (2023). doi:10.3389/fphy.2023.1166566

[124] J. Gunst, Y.A. Litvinov, C.H. Keitel et al., Dominant secondary nuclear photoexcitation with the x-ray free-electron laser. Physical Review Letters **112**, 082501 (2014). doi:10.1103/PhysRevLett.112.082501

[125] Y. Wu, J. Gunst, C.H. Keitel et al., Tailoring laser-generated plasmas for efficient nuclear excitation by electron capture. Physical review letters **120**, 052504 (2018). doi:10.1103/PhysRevLett.120.052504

[126] J. Qi, B. Liu, X. Wang, Laser-based approach to verify nuclear excitation by electron capture. Phys. Rev. C **110**, L051601 (2024). doi:10.1103/PhysRevC.110.L051601

[127] J. Qi, H. Zhang, X. Wang, Isomeric excitation of ^{229}Th in laser-heated clusters. Physical Review Letters **130**, 112501 (2023). doi:10.1103/PhysRevLett.130.112501

[128] A.P. Andre Junker, C.H. Keitel, Cooperative effects in nuclear excitation with coherent x-ray light. New Journal of Physics **14**, 085025 (2012). doi:10.1088/1367-2630/14/8/085025

[129] J. Feng, W. Wang, C. Fu et al., Femtosecond pumping of nuclear isomeric states by the coulomb collision of ions with quivering electrons. Physical Review Letters **128**, 052501 (2022). doi:10.1103/PhysRevLett.128.052501

[130] A. Afanasev, V.G. Serbo, M. Solyanik, Radiative capture of cold neutrons by protons and deuteron photodisintegration with twisted beams. Journal of Physics G: Nuclear and Particle Physics **45**, 055102 (2018). doi:10.1088/1361-6471/aab5c5

[131] A. Afanasev, C.E. Carlson, A. Mukherjee, Recoil momentum effects in quantum processes induced by twisted photons. Physical Review Research **3**, 023097 (2021). doi:10.1103/PhysRevResearch.3.023097

[132] A. Afanasev, C.E. Carlson, Delta baryon photoproduction with twisted photons. Annalen der Physik **534**, 2100228 (2022). doi:10.1002/andp.202100228

[133] Z.W. Lu, L. Guo, Z.Z. Li et al., Manipulation of giant multipole resonances via vortex γ photons. Physical Review Letters **131**, 202502 (2023).

doi:10.1103/PhysRevLett.131.202502
[134] P.O. Kazinski, A.A. Sokolov, Excitation of multipolar transitions in nuclei by twisted photons. Physics of Atomic Nuclei **87**, 561–569 (2024). doi:10.1134/S1063778824700364
[135] M. Uchida, A. Tonomura, Generation of electron beams carrying orbital angular momentum. nature **464**, 737–739 (2010). doi:10.1038/nature08904
[136] J. Verbeeck, H. Tian, P. Schattschneider, Production and application of electron vortex beams. Nature **467**, 301–304 (2010). doi:10.1038/nature09366
[137] B.J. McMorran, A. Agrawal, I.M. Anderson et al., Electron vortex beams with high quanta of orbital angular momentum. science **331**, 192–195 (2011).
[138] C.W. Clark, R. Barankov, M.G. Huber et al., Controlling neutron orbital angular momentum. Nature **525**, 504–506 (2015). doi:10.1038/nature15265
[139] A. Luski, Y. Segev, R. David et al., Vortex beams of atoms and molecules. Science **373**, 1105–1109 (2021). doi:10.1126/science.abj2451
[140] P. Zhao, I.P. Ivanov, P. Zhang, Decay of the vortex muon. Physical Review D **104**, 036003 (2021). doi:10.1103/PhysRevD.104.036003
[141] H. Larocque, I. Kaminer, V. Grillo et al., Twisting neutrons may reveal their internal structure. Nature Physics **14**, 1–2 (2018). doi:10.1038/nphys4322x
[142] I. Kaminer, J. Nemirovsky, M. Rechtsman et al., Self-accelerating dirac particles and prolonging the lifetime of relativistic fermions. Nature Physics **11**, 261–267 (2015). doi:10.1038/nphys3196
[143] I. Madan, G.M. Vanacore, S. Gargiulo et al., The quantum future of microscopy: Wave function engineering of electrons, ions, and nuclei. Applied Physics Letters **116**, 230502 (2020). doi:10.1063/1.5143008
[144] S. Franke-Arnold, Optical angular momentum and atoms. Philosophical Transactions of the Royal Society A: Mathematical, Physical and Engineering Sciences **375**, 20150435 (2017). doi:10.1098/rsta.2015.0435
[145] A. Afanasev, C.E. Carlson, M. Solyanik, Atomic spectroscopy with twisted photons: Separation of M1-E2 mixed multipoles. Physical Review A **97**, 023422 (2018). doi:10.1103/PhysRevA.97.023422
[146] A. Afanasev, C.E. Carlson, C.T. Schmiegelow et al., Experimental verification of position-dependent angular-momentum selection rules for absorption of twisted light by a bound electron. New Journal of Physics **20**, 023032 (2018). doi:10.1088/1367-2630/aaa63d
[147] S.L. Schulz, S. Fritzsche, R.A. Müller et al., Modification of multipole transitions by twisted light. Physical Review A **100**, 043416 (2019). doi:10.1103/PhysRevA.100.043416
[148] A.V. Afanasev, D. Karlovets, V. Serbo, Schwinger scattering of twisted neutrons by nuclei. Physical Review C **100**, 051601 (2019). doi:10.1103/PhysRevC.100.051601
[149] A. Afanasev, D. Karlovets, V. Serbo, Elastic scattering of twisted neutrons by nuclei. Physical Review C **103**, 054612 (2021). doi:10.1103/PhysRevC.103.054612
[150] K. Yao, Z. Geng, J. Xiao et al., KLL dielectronic recombination resonant strengths of He-like up to O-like xenon ions. Phys. Rev. A **81**, 022714 (2010). doi:10.1103/PhysRevA.81.022714
[151] Z. Hu, G. Xiong, Z. He et al., Giant retardation effect in electron-electron interaction. Phys. Rev. A **105**, L030801 (2022). doi:10.1103/PhysRevA.105.L030801
[152] Z. Huang, S. Wang, W. Wen et al., Absolute dielectronic recombination rate coefficients of highly charged ions at the storage ring CSRm and CSRe. Chinese Physics B **32**, 073401 (2023). doi:10.1088/1674-1056/acbc69
[153] G. Xiao, J. wen Xia, Y. Yuan et al., Overview on the hirfl-csr facility. International Journal of Modern Physics E-nuclear Physics **18**, 405–410 (2009).
[154] Y. Yang, Y. Wang, Z. Ma et al., Feasibility of probing the neec process using storage rings. Frontiers in Physics **12**,. doi:10.3389/fphy.2024.1410076
[155] X. Zhou, J. Yang, t.H.p. team, Status of the high-intensity heavy-ion accelerator facility in china. AAPPS Bulletin **32**, 35 (2022). doi:10.1007/s43673-022-00064-1
[156] T. Schenkel, A. Hamza, A. Barnes et al., Interaction of slow, very highly charged ions with surfaces. Progress in Surface Science **61**, 23–84 (1999). doi:https://doi.org/10.1016/S0079-6816(99)00009-X
[157] R.A. Snavely, B. Zhang, K. Akli et al., Laser generated proton beam focusing and high temperature isochoric heating of solid matter. Physics of Plasmas **14**, 092703 (2007). arXiv:https://pubs.aip.org/aip/pop/article-pdf/doi/10.1063/1.2774001/1355 doi:10.1063/1.2774001
[158] M. Imai, M. Sataka, K. Kawatsura et al., Equilibrium and non-equilibrium charge-state distributions of 2mev/u sulfur ions passing through carbon foils. Nuclear Instruments and Methods in Physics Research Section B: Beam Interactions with Materials and Atoms **267**, 2675–2679 (2009). Proceedings of the 23rd International Conference on Atomic Collisions in Solids. doi:https://doi.org/10.1016/j.nimb.2009.05.035
[159] R.A. Wilhelm, The charge exchange of slow highly charged ions at surfaces unraveled with freestanding 2d materials. Surface Science Reports **77**, 100577 (2022). doi:https://doi.org/10.1016/j.surfrep.2022.100577
[160] C.J. Chiara, J.J. Carroll, M.P. Carpenter et al., Reply to: Possible overestimation of isomer depletion due to contamination. Nature **594**, E3–E4 (2021). doi:10.1038/s41586-021-03334-4
[161] D. Lu, Y. Yang, J. Xiao et al., Upgrade of the electron beam ion trap in shanghai. Review of Scientific Instruments **85**, 093301 (2014). doi:10.1063/1.4894212